Fission of heavy nuclei induced by energetic pions

K. H. Hicks,* R. G. Jeppesen, J. J. Kraushaar, P. D. Kunz, R. J. Peterson,
R. S. Raymond,† R. A. Ristinen, and J. L. Ullmann
Nuclear Physics Laboratory, Department of Physics, University of Colorado, Boulder, Colorado 80309

F. D. Becchetti
Department of Physics, University of Michigan, Ann Arbor, Michigan 48109

J. N. Bradbury and M. Paciotti
Los Alamos National Laboratory, Los Alamos, New Mexico 87545
(Received 13 November 1984)

Fission of ^{238}U, ^{209}Bi, and ^{197}Au induced by both positive and negative pion beams at incident energies of 60 to 100 MeV is examined. Energy and mass spectra and angular correlations of coincident fission fragments are compared to theoretical calculations and to other data. Excitation energies of the fissioning system in excess of 100 MeV are deduced, implying that the fission examined in this study is caused primarily by true absorption of the pion. The masses of the coincident fission fragments are found to have a wider distribution than those from fissioning systems of similar excitation energy induced by nucleon beams. The fission cross sections are close to the reaction cross sections for ^{238}U and scale with the fissility for the other nuclei studied.

I. INTRODUCTION

Recent interest has been directed to the question of how the primary pion-nucleus interaction couples to collective modes of nuclei. Resolution of this question requires knowledge of all parts of the pion-nucleus reaction cross section, σ_R, that could lead to collective nuclear excitations. A thorough presentation of data on the component parts of the reaction cross section σ_R as they depend on both target mass and pion beam energy has been published by Ashery *et al.*[1] Theoretical calculations of σ_R and its component parts have used pion optical models with a modified Kisslinger potential.[2,3] In the present work we have investigated the pathways which lead from the primary pion-nuclear interaction through a compound system to decay by fission.

Fission is a well-understood decay mode for heavy nuclei. An extensive review of fission studies involving a number of targets and projectiles is given by Vandenbosch and Huizenga.[4] However, published data on fission induced by energetic pions are scant. Data for fission induced by 300 MeV π^+ incident on ^{238}U were reported[5] in 1958 when pion beams first became available. More recent published data[6] have been limited to results from stopped π^-. No comprehensive report for fission induced by both π^+ and π^- over a range of energies has been published.

The energy range of 60 to 100 MeV was selected for the present study on the basis of calculations[7] of the pion mean free path, λ, in nuclear matter. A pion with $\lambda < 1$ fm, as expected at the delta resonance energy near 175 MeV, is less likely to interact with the entire nuclear volume than is a 70 MeV pion with $\lambda \simeq 4$ fm. Study of the nucleus as a collective body is thus well suited to this lower energy range.

One goal of the present study was to determine whether there is a difference between the fission process induced by energetic pions and conventional fission as induced by neutrons or light-ion beams. A difference could indicate reaction mechanisms leading to collective phenomena that are specific to the pion-nuclear interaction. In order to make a comparison with conventional fission, it is necessary that the excitation energy of the compound nucleus be determined, because fission is known to be sensitive to this quantity. Hence, we first examine the kinetic features of pion-induced fission.

Measured energy and mass spectra of the fission fragments were analyzed in terms of the model formulated by Nix[8] to infer the excitation energy of the fissioning system. These measurements and analysis are described in subsection A of the following sections. From the analysis, it is deduced that the main contribution to pion-induced fission is from true absorption of the pion which deposits considerable excitation energy in the compound nucleus.

In a second experiment, pion-induced fission cross sections were measured. The measurements and analysis are described in subsection B of the following sections. These fission cross sections can be compared to those for fission induced by protons at a beam energy that leaves the compound nucleus with an excitation energy similar to the rest mass of the pion. From this comparison, we conclude that fission induced by pions is similar to conventional nucleon-induced fission, with the exception that the masses of the fission fragments have a much wider distribution for pion-induced fission.

The present study differs from earlier fission measurements in two important respects. First, the availability of beams of pions of either charge state makes possible an experimentally consistent examination both of the isospin dependence of projectile-nucleus interactions leading to

fission, and of fission of compound nuclear systems differing only by two units of charge and produced from the same target isotope. Second, as compared to other energetic hadronic projectiles, the small mass, zero intrinsic angular momentum, and true absorption process of the pion can lead to fission from a state of relatively low angular momentum and high excitation energy.

II. EXPERIMENTAL METHODS

A. The LAMPF Biomedical Channel

The measurements of fission fragment energies and masses were made at the Biomedical Channel of the Clinton P. Anderson Meson Physics Facility (LAMPF). These measurements will be referred to as data set *A*. The incident pion kinetic energies in the laboratory for these data were 65, 78, and 96 MeV. The pion beam intensity was monitored with an ion chamber that enabled relative normalization. An array of eight thin ($<150\ \mu$m) silicon detectors was placed in the scattering chamber on either side of the target to detect coincident fission fragments. The targets used were depleted ($>99.8\%$ enriched) ^{238}U (0.430 mg/cm^2), ^{209}Bi (1.20 mg/cm^2), and ^{197}Au (0.844 mg/cm^2). Energy and timing signals for both fragments were recorded with standard electronics. The energy signals were calibrated by using a thin ^{252}Cf source. The instrumental coincident timing resolution was less than 2 ns (determined by using a pulser) and the energy signal was calibrated within ±0.3 MeV at 185 MeV (using appropriate pulse-height defect corrections[9]).

Total contributions to the measured ^{238}U fission rates from particles other than pions were determined to be less than 1% of the measured events. Protons were removed from the pion beam by an absorber in the channel. Electron and muon contaminants are known from time-of-flight measurements to be each only about 10% of the pion flux for the channel tunes used in this experiment, and the lepton-induced fission cross sections for ^{238}U (or ^{235}U) are no more than about 2% of the pion-fission cross sections.[10] Thus no more than about 0.2% of the measured events were due to electrons or muons.

Neutron fluxes were measured for both pion beam polarities at points 0.5 and 1.4 m from the beam axis in a plane perpendicular to the beam axis and intersecting the target location. These measurements were made using a Bonner sphere method previously described.[11] The measurements showed that there were typically 10^3 to 10^4 neutrons/s cm^2 near (and presumably at) the target location as compared to the incident pion flux of typically 10^7 to 10^8/s cm^2 on the target. The neutron flux was found to be divided roughly equally into three energy bins, $E_n<1$ eV, 1 eV $<E_n<10$ keV, and $E_n>10$ keV. Thus it may be concluded that the fast neutron fissions of ^{238}U were no more than 0.1% relative to the pion fissions, assuming the same geometric cross sections for both reactions. Fission events due to slow neutrons on the ($<0.2\%$) ^{235}U in the target are estimated not to exceed 0.1% of the pion fission of ^{238}U, even considering the 10^3 times greater than geometric fission cross section of ^{235}U for slow neutrons.

Absolute cross section measurements were not made at the Biomedical Channel because of uncertainties in absolute normalization of the pion beam on the target.

B. The LAMPF LEP Channel

The relative fission cross section measurements for data set *A* were normalized and extended by a second experiment at the low-energy pion (LEP) line at LAMPF. These measurements will be referred to as data set *B*. The incident pion laboratory kinetic energies were 60, 70, 80, 90, and 100 MeV. The pion beam flux was measured by using the ^{12}C($\pi^{\pm},\pi$N)^{11}C reaction and absolute counting of the radioactive ^{11}C decay. This technique has been described by Butler *et al.*[12] The targets used were depleted ^{238}U (0.630 mg/cm^2) and ^{209}Bi (0.744 mg/cm^2). Track detector techniques[13] were used to measure the fission fragment yield from these targets. The track detector material Cronar[14] was mounted in the scattering chamber on two circular arcs subtending angles of 160° on either side of the target at a radius of 15.1 cm. The exposed Cronar was etched in a 6.25 *M* solution of KOH for approximately 3 h. The solution was kept at 68 °C and stirred continuously.

The muon contamination of the pion beam at LEP is small ($<10\%$) and is not expected to contribute more than 0.2% to the fission cross section, as for data set *A*. The electron contaminant flux, although larger ($\simeq1$ e$^-/\pi^-$ at 60 MeV and $\simeq0.1$ e$^-/\pi^-$ at 100 MeV) is still expected[10] to contribute only about 2% to the fission cross section at 60 MeV and less than 0.3% at 100 MeV. The proton contamination of the π^+ beam was eliminated by an absorber in the beam channel.

The flux of energetic and thermal neutrons in the LEP beam is expected to be $<10^{-4}$ of the pion flux from channel design specifications. This will contribute less than 0.1% to the measured fission rate for the depleted ^{238}U target, as for data set *A*. The expected negligible contribution from neutrons of all energies was confirmed by Bonner sphere measurements near the target, and by measuring the fission rate when the ^{238}U target and detector array were displaced 10 cm from the pion beam.

III. DATA

A. Energy and mass measurements

The measurements from data set *A* are summarized for 78 MeV π^+ incident on ^{238}U in the spectra shown in Fig. 1. The energy spectrum from one detector is shown in Fig. 1(a). Fission fragments are easily distinguished from the light ions that have only a small energy loss in passing through the thin detectors. The relative time between detection of the two fission fragments is shown in Fig. 1(b). The sum of the energy signals from two coincident detectors results in the total kinetic energy, E_T, spectrum shown in Fig. 1(c). In Fig. 1(d), the correlation between the signals of Fig. 1(b) and (c) is shown; the low energy signals are randomly distributed in time and the fission fragment signals are well separated from this background. Similar spectra are seen in Fig. 2 for 78 MeV π^+ incident

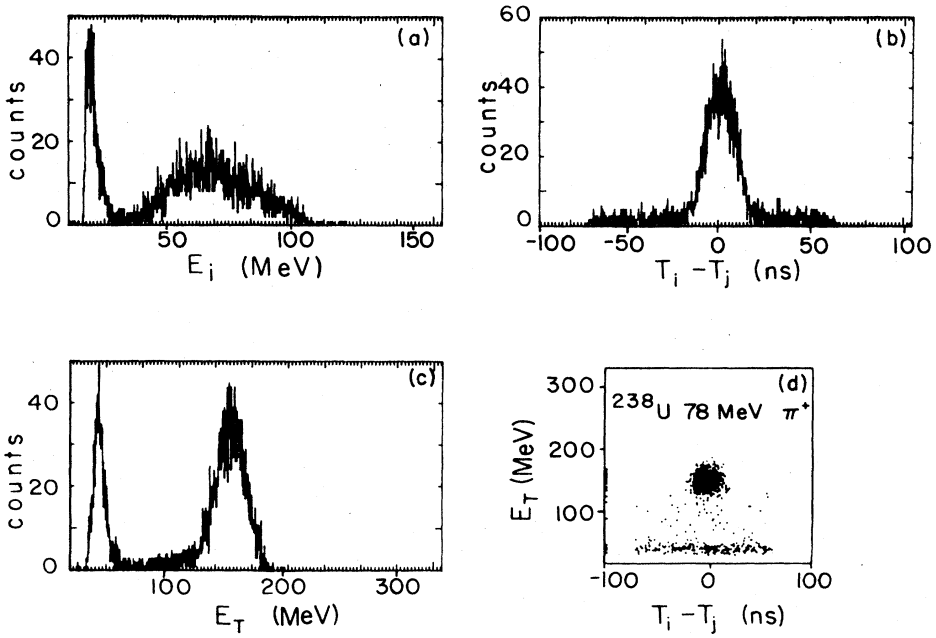

FIG. 1. Data for 78 MeV π^+ incident on ^{238}U: (a) energy spectrum of one fission counter for coincidence events, (b) relative timing between two counters giving an event, (c) total kinetic energy spectrum of the two coincident fission fragments, and (d) two-dimensional plot of the total kinetic energy versus the time-of-flight difference.

on ^{209}Bi; the results for ^{197}Au are similar but are not shown here.

The parameters of particular interest for later comparison with calculations are the average values of E_T and widths ΔE_T. These parameters can be represented by the centroid and the full width at half maximum (FWHM) of a Gaussian fit to the summed fission fragment energy peak. These values are listed in Table I for the targets and beam energies used in data set A. It is of interest to note that there are essentially no counts above about 200 MeV in the E_T spectra. This shows that the absorbed pion rest mass is not manifested in kinetic energy of the fission fragments.

The mass distributions for the fission fragments can be

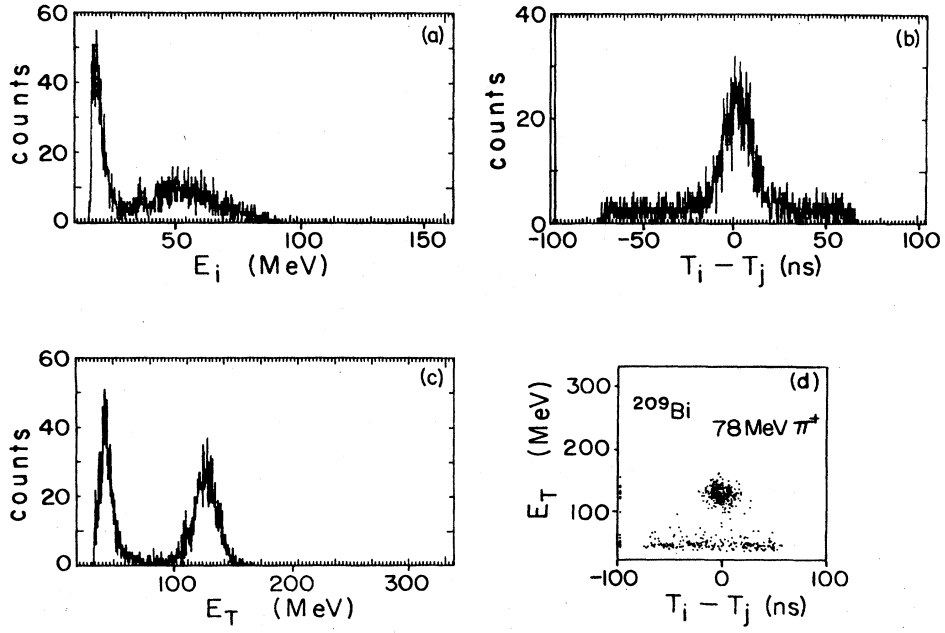

FIG. 2. Data for 78 MeV π^+ incident on ^{209}Bi. Parts (a)—(d) are as in Fig. 1.

TABLE I. Comparison of measured and calculated values for the mean total kinetic energy E_T and its width, ΔE_T, and for the width of the mass distributions. The calculated values assume a compound nucleus of the target plus the pion and an excitation energy resulting from true absorption of the pion. All terms are defined in the text.

Target	Beam	T_π (MeV)	E_T[a](exp) (MeV)	ΔE_T[a](exp) (MeV)	ΔM[b](exp) (u)	E_T(calc) (MeV)	E^*_{SP} (MeV)	θ (MeV)	ΔE_T(calc) (MeV)	ΔM(calc) (u)
^{252}Cf			186.5±0.3	28.8±0.6		185.0		0.0	(25.5)[c]	
^{238}U	π^+	65	167.4±0.4	30.7±0.8	67.5±1.2	171.6	183	2.50	28.8	46.6
		78	164.9±0.3	29.3±0.5	66.2±1.2	171.6	196	2.58	29.1	47.4
		96	167.9±0.3	31.2±0.6	65.5±1.4	171.6	214	2.70	29.7	48.3
	π^-	65	161.8±0.3	27.3±0.5	63.3±1.7	165.3	216	2.17	28.6	46.8
		78	161.4±0.2	27.2±0.3	66.2±1.9	165.3	229	2.79	29.0	47.5
		96	161.9±0.4	27.4±0.8	62.8±1.4	165.3	247	2.90	29.4	48.4
^{209}Bi	π^+	78	142.9±0.3	23.6±0.6	60.6±1.5	149.5	190	2.72	26.4	41.7
^{197}Au	π^+	65	141.6±3.1			140.0				
		78	141.2±1.0	21.6±3.0	46.5±3.3	140.0	187			
		96	141.8±0.9	24.8±1.5	48.7±2.8	140.0	205	2.91	27.1	42.0
	π^-	65	(120.0±10)			134.2				
		78	136.3±4.7			134.2				
		96	132.5±2.8			134.2				

[a] Values are corrected for fission fragment energy loss in the target. Only fitting errors are listed; errors not included are ±0.3 MeV for calibration; ±0.7 MeV for pulse height defect corrections; and ±0.9, ±3.0, and ±0.8 MeV for ^{238}U, ^{209}Bi, and ^{197}Au, target thickness corrections, respectively. Corrections have not been made for post-fission neutron emission.

[b] Only fitting errors are listed; an additional overall error of ±0.7 MeV due to calibration and pulse height defect uncertainties is not included.

[c] For targets with Z^2/A greater than that of ^{238}Np, the calculations of Nix (Ref. 8) become of questionable accuracy.

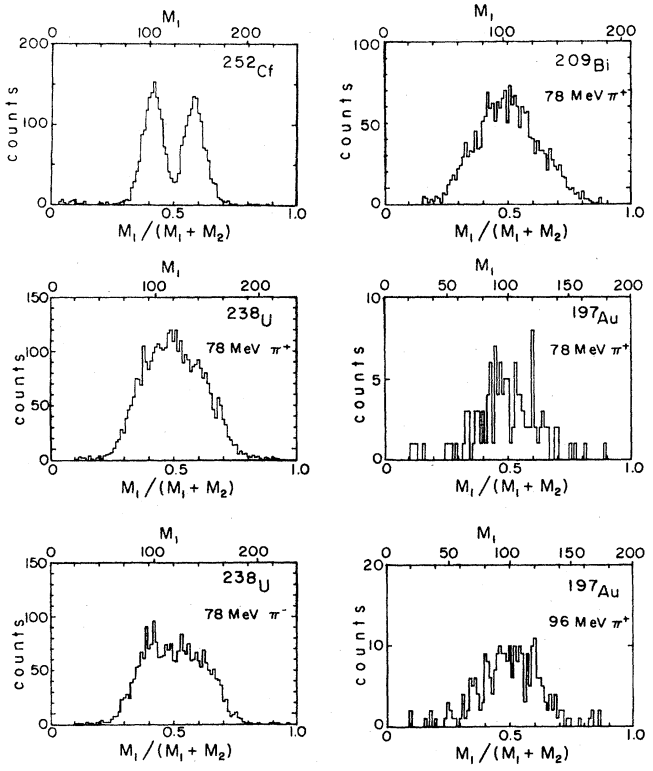

FIG. 3. Mass distributions of the fission fragments as deduced using Eq. (1).

deduced from the energy measurements by using the approximate relation[15]

$$\frac{M_1}{M_1+M_2}\simeq\frac{E_2}{E_1+E_2}\ , \tag{1}$$

where the subscripts refer to one or the other of the binary fission fragments having mass M or kinetic energy E. The mass distributions obtained in this way for spontaneous fission of ^{252}Cf and for samples of data set A are shown in Fig. 3. To produce these data, gates were set on the fission fragment peaks in the relative timing and total kinetic energy spectra [see Figs. 1(d) and 2(d)]. The widths of the mass distributions, ΔM, as given by the FWHM for a Gaussian fit, are also listed in Table I for later comparison with calculations.

The angular correlations of the fission fragments for 96 MeV π^+ incident on ^{238}U and ^{197}Au are shown in Figs. 4(a) and (b), where Gaussian fits have been drawn through the data. The centroids of these fits are close to the values indicated for full linear momentum transfer (FLMT) of the incident pion momentum; this is expected and observed for conventional fission process.[9] The widths of these angular correlations are determined mainly by the angular resolution of the experimental setup which was limited by the beam spot size, typically 5 cm in diameter.

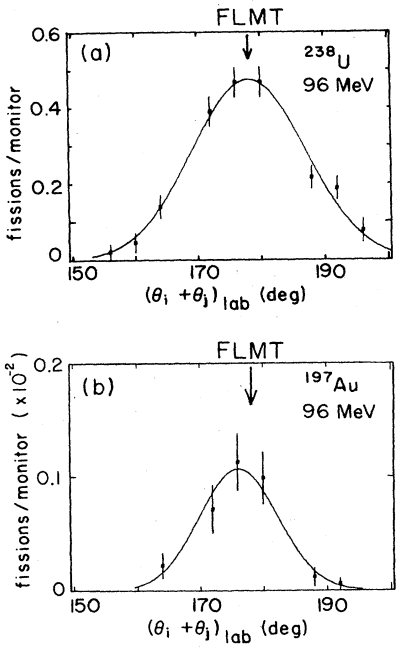

FIG. 4. Angular correlations for 96 MeV π^+ incident on (a) ^{238}U and (b) ^{197}Au. Arrows have been placed at the angles calculated for full linear momentum transfer (FLMT).

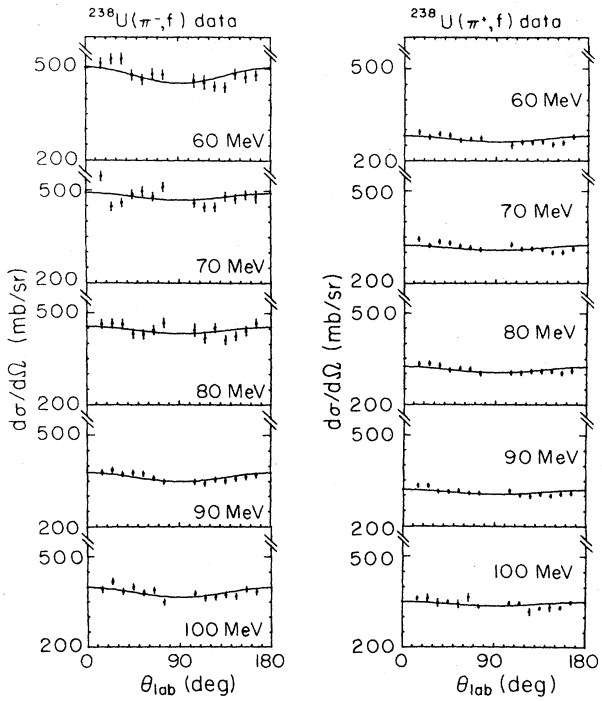

FIG. 5. Angular distributions of the fission fragments for a range of π^+ and π^- energies. The curves are fit to the function $A(1+B\cos^2\theta)$ where A and B are given in Table II.

B. Fission cross sections

Differential cross sections for fission of ^{238}U induced by π^- and π^+ at the incident energies used for data set B are shown in Figs. 5(a) and (b). An angular distribution of the form

$$W(\theta)=A(1+B\cos^2\theta) \tag{2}$$

is expected[16,4] for conventional fission. A fit to the data with this functional form is shown by the solid curves in Fig. 5. Only statistical errors are plotted in this figure. The angular distributions are nearly isotropic as expected[17] for conventional fission, especially for a high excitation energy of the fissioning nucleus. The total fission cross sections, σ_F, were obtained by integrating the angular distribution over solid angle to give

$$\sigma_F=\frac{4\pi}{2}A\left[1+\frac{B}{3}\right], \tag{3}$$

where the factor of 2 in the denominator is because there are two fission fragments per event. The values determined for A, B, and σ_F are listed in Table II, where the small values for B are consistent with expectations for the low momentum pion beams.

IV. ANALYSIS

A. Energy and mass distributions

The total kinetic energy release for binary fission induced by many different projectiles and beam energies has been tabulated for a range of targets.[18] From this compilation it is seen that the average value of the fission fragment total kinetic energy can be described by

$$\langle E_T\rangle=\left[0.1071\frac{Z^2}{A^{1/3}}+22.2\right]\text{ MeV} \tag{4}$$

for all of the data (Z and A refer to the charge and mass number of the compound nucleus). The compound nucleus for fission induced by pions will initially have the A of the target nucleus, and either the Z of the target nucleus for inelastic scattering leading to fission, or $Z\pm1$ for true absorption of the $\pi^\pm$. However, the values of A and Z may change by a few percent for heavy nuclei due to preequilibrium emission of particles. The calculated values $\langle E_T(\text{calc})\rangle$ are listed in Table I under an assumption of true absorption of the pion. These calculated values agree rather well with the measured values of E_T, also in Table I. This is the first part of the evidence that the fission studied here stems mainly from true absorption of the pion, in that the charge of the fissioning system is determined from the data on fission fragment kinetic energy.

The model formulated by Nix[8] has proven adequate in predicting the widths of both the total kinetic energy and mass distributions of the fission fragments for conventional fission. In Nix's model, these widths can be described by

$$\Delta E_T(\text{calc})=(\text{FWHM})_E\times[\coth(\hbar\omega_4/2\theta)]^{1/2} \tag{5a}$$

and

TABLE II. Total fission cross sections, σ_F, along with the constants used in Eq. (3).

Target	Beam	T_π (MeV)	A (b)	B	σ_F[a] (b)
^{238}U	π^-	60	0.453	0.113	2.96±0.37
		70	0.470	0.049	3.00±0.30
		80	0.434	0.051	2.77±0.28
		90	0.349	0.083	2.26±0.23
		100	0.366	0.090	2.36±0.24
	π^+	60	0.262	0.070	1.68±0.17
		70	0.308	0.049	1.97±0.20
		80	0.305	0.063	1.96±0.20
		90	0.305	0.049	1.94±0.19
		100	0.337	0.041	2.14±0.21
^{209}Bi	π^-	80	0.0147	0.096	0.10±0.01
	π^+	80	0.0438	0.001	0.276±0.028

[a] Uncertainties are $<5\%$ for statistical and fitting errors, $<7\%$ for pion beam flux normalization ($\simeq 10\%$ for 60 MeV π^-), and 5% for target thickness.

$$\Delta M(\text{calc}) = (\text{FWHM})_A \times [\coth(\hbar\omega_3/2\theta)]^{1/2} , \quad (5b)$$

where $(\text{FWHM})_E$, $(\text{FWHM})_A$, $\hbar\omega_3$, and $\hbar\omega_4$ are constants for a given compound nucleus and θ is the nuclear temperature at the saddle point (the nuclear temperature is related in general to the excitation energy E^* by[8] $E^* = a\theta^2 - \theta$, where $a = A/8$ MeV^{-1} is the level density parameter). Nix compares[8] the calculated ΔE_T and ΔM widths with the values observed for fission induced by many different projectiles and energies from a range of targets. These widths are plotted versus the fissility in Figs. 19 and 20 of Ref. 8. The ΔE_T and ΔM widths from several sources,[8] divided by the bracketed terms in Eqs. (5a) and (5b), fall into a definite line for both the ΔE_T and ΔM widths in these figures. The ΔE_T data of Ref. 8 are described nicely by Nix's calculations, although the calculated $(\text{FWHM})_E$ are about 20% lower than the data. The calculated $(\text{FWHM})_A$ do not follow the data; however, an empirical value of $(\text{FWHM})_E$ can be extracted by drawing a smooth line through the data plotted in Ref. 8. A value of $(\text{FWHM})_A$ can be obtained in a similar fashion.

Using these phenomenological values of $(\text{FWHM})_E$ and $(\text{FWHM})_A$, and the $\hbar\omega_4$ and $\hbar\omega_3$ given by Nix, the widths for ΔE_T and ΔM can be calculated for a given excitation energy of the compound nucleus. The excitation energy at the saddle point for fission induced by pions is given, under an assumption of true absorption of the pion, by

$$E^*_{\text{SP}} = m_\pi c^2 + T_\pi - E_f \pm V_C , \quad (6)$$

where $m_\pi c^2$ is the rest mass of the pion, T_π is the pion kinetic energy, E_f is the fission barrier, and V_C is the Coulomb barrier. The computed E^*_{SP}, and the resulting predicted ΔE_T and ΔM from Nix's model, are listed in Table I, where the (small) correction for preequilibrium nucleon emission has not been included.

The ΔE_T(calc) widths for pion-induced fission of ^{238}U correspond remarkably well to the measured ΔE_T widths in Table I. Thus the assumption of true absorption of the pion used for the excitation energy in this calculation seems to be reasonable. In general, the measured ΔE_T widths for ^{238}U plus π^+ appear to be consistently 1 MeV higher than the calculated width ΔE_T, and for ^{238}U plus π^- the measured ΔE_T values are consistently 1 MeV lower than the calculated ΔE_T values. A larger width corresponds to a higher excitation energy, and a smaller width corresponds to a lower excitation energy. Because the shape of the curve compared to the data in Fig. 20 of Ref. 8 is fixed to the shape calculated by Nix, a relative comparison of the zero-temperature energy widths $(\text{FWHM})_E$ for different nuclei would likely have less error than the absolute errors in normalizing the curve to the data. Assuming small relative errors for the calculated ΔE_T values, a conclusion may be reached, based on the Nix calculations, that for ^{238}U the π^+ deposits more excitation energy in the nucleus than does the π^-. However, the Nix calculations become of questionable accuracy for nuclei heavier than ^{238}Np, and so this conclusion may be questioned.

The measured ΔE_T widths for ^{209}Bi and ^{197}Au are somewhat less than the calculated ΔE_T. The excitation energy corresponding to these measured widths can be extracted with the result that for both nuclei a nuclear temperature of $\theta \simeq 2.1$ MeV is needed to match the calculations to the measured widths. This value of θ corresponds to an excitation energy of about 100 MeV. This indicates that most of the fission processes are initiated by true absorption, followed by emission of a few nucleons.

The measured mass widths ΔM given in Table I are seen to be consistently larger than the calculated ΔM widths for all targets. A larger mass width corresponds to a higher excitation energy. This result is surprising in light of the excitation energies of about 100–200 MeV deduced from the comparison between the energy widths measured and those calculated (the same temperature θ was used to calculate both the ΔE energy widths and these

ΔM mass widths). The phenomenological ΔM widths assume the temperature dependence predicted by Nix, even though the calculated curve in Ref. 8 does not follow the trend of the data. However, because the data in Ref. 8 cover a wide range of excitation energies, it is reasonable to assume that the procedure used to divide out the temperature dependence should be valid at the excitation energies resulting from pion absorption. Nonetheless, the nuclear temperatures needed to fit the mass widths ΔM measured in this study along with the other data in Ref. 8 are unreasonably high (4 to 5.5 MeV). A direct comparison of the ΔM given in Table I to the mass width for fission of ^{238}U induced by 150 MeV protons,[19] measured as 52 ± 1 u, shows the ΔM for ^{238}U plus π^+ to be about 13 u larger. Furthermore, the mass width for fission of ^{197}Au induced by[20] 45 MeV ^{3}He, measured as 31 ± 1 u, compares closely with the predicted width of $\Delta M = 30$ u. Because the same methods (even the same detectors) were used for those earlier ^{3}He measurements and the present study, one might expect similar reliability in extracting the mass widths for the present results. Hence, the conclusion is reached, based on direct comparisons with other data and on the Nix calculations, that the fission fragment masses are more widely distributed for fission induced by pions than for fission induced by light ions.

B. Total fission cross sections

The total fission cross sections from data set *B* may also be compared with cross sections for fission induced by protons at beam energies greater than 140 MeV ($=m_\pi c^2$). This comparison is most easily seen when the fission cross sections are divided by their respective reaction cross sections, σ_R. The values of σ_F listed in Table II for incident pions at 80 MeV were divided by the σ_R calculated with the pion optical model using parameter set *C* of Stricker, Carr, and McManus.[21] The resulting values are plotted along with the data for 156 MeV (Ref. 22) and 190 MeV (Ref. 23) protons in Fig. 6. Also plotted in Fig. 6 are points in parentheses for pion-induced fission of ^{197}Au. These points were obtained by normalizing the values of the σ_F for ^{238}U at 78 MeV from data set *A* to the σ_F for ^{238}U from data set *B* at 80 MeV; using this normalization factor in conjunction with the relative values from the beam monitor in the setup for data set *A*, the σ_F for ^{197}Au at 78 MeV was obtained. The parentheses around these points denote the indirect normalization method for ^{197}Au. The data in Fig. 6 for pions have been plotted assuming a *Z* and *A* of the compound nucleus resulting from true absorption. Under this assumption, the data for both pions and protons agree quite nicely for equivalent excitation energies available from the beams.

Calculations of pion-induced fission cross sections were accomplished in two sequential steps. The first follows the initial interaction of the pion with the nucleus through to a thermally equilibrated nucleus and the second determines the probability of fission for this nucleus. The validity of this approach rests on the success of present calculations of pion-nucleus interactions (for the first part), the success of statistical fission calculations (for the second part), and the connection between the two parts as discussed in the following.

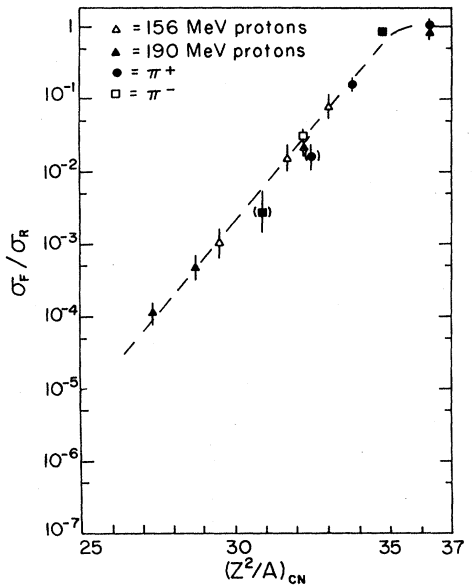

FIG. 6. Comparison of the proton-induced fission data at 156 MeV (Ref. 22) and 190 MeV (Ref. 23) with the pion-induced fission data at 80 MeV from the present study. The dashed line guides the eye.

One of the main assertions from the present data on average kinetic energy release, angular corrections, and angular distributions of the fission fragments is that fission induced by a beam of energetic pions is not much different from fission induced by a nucleon beam that leaves the nucleus with similar excitation energy. A basic assumption in calculations for nucleon-induced fission is that the nucleus is in thermal (statistical) equilibrium when fission occurs. Thus, because no unusual mechanism for pion-induced fission was observed, there seems to be no problem in connecting the two parts of the calculations already described. The two calculations presented in the following are either based on the cascade model or the optical model in conjunction with statistical fission calculations by the computer program ALICE.[24]

Cascade calculations have been successful in predicting general features of fast emitted particles.[25] The pion cascade code ISOBAR (Ref. 26) was used to thermalize the nucleus in the calculations presented here. Although ISOBAR has done well in reproducing pion-nucleus cross section data[26] near delta resonance energies, the code is largely untested in the 60 to 100 MeV energy range. Furthermore, ISOBAR assumes that all pion-nucleon interactions proceed through the Δ resonance, without inclusion of *s*-wave interaction terms. Nonetheless, ISOBAR is possibly the best pion cascade code presently available. The output from ISOBAR gives the excitation energy, E^*, and angular momentum, *J*, of the residual nuclei. These values of E^* and *J* were used in fission calculations with the ALICE code using only the option for the standard Bohr-Wheeler model with fission-neutron emission competition and fission barriers from the rotating liquid-drop model. The results of these calculations for ^{238}U are presented in Figs. 7(a) and (b) for two values of the level density ratio,

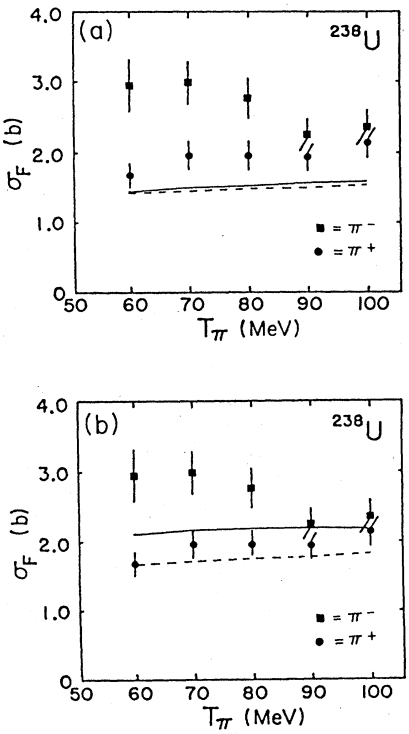

FIG. 7. Comparison of the fission cross section for ^{238}U to calculations for π^- (solid line) and π^+ (dashed line) using the ISOBAR and ALICE codes with values of the level density ratio $R = a_f/a_\nu$ equal to (a) 1.0 and (b) 1.1.

$R = a_f/a_\nu$. This parameter, R, represents the ratio of the density of levels at a given excitation energy above the saddle point to the level density at an equivalent excitation energy above the ground state. In the Fermi gas model, $R = 1$ with $a_f = a_\nu \simeq A/9$ MeV^{-1}. The value of $a_f = a_\nu$ used in Fig. 7(a) predicts that the fission cross sections of ^{238}U are approximately equal for both incident π^+ and π^-. The reason for this is that the reduction in the fissility due to a decrease in charge for π^- incident on ^{238}U just offsets the increase in σ_R for π^- (also a Coulomb effect). Clearly, this does not reproduce the data well. Better agreement is obtained for $R = 1.1$ as shown in Fig. 7(b). This latter value was found necessary to reproduce the data of ^{4}He incident on ^{233,234,235}U targets.[27] Good fits to those data are obtained only for values of $R > 1.1$, suggesting that the levels are compressed over the fission barrier. Even better agreement might be obtained by adjusting the fission barriers used in the ALICE. These would on the average need to be slightly lower (by 10 to 20%) than the fission barriers calculated from the liquid drop model with shell corrections. However, experimental fission barriers are not known for many of the nuclei from which fission takes place (the compound nucleus may emit several neutrons or protons before fissioning). Similar modifications to the code would be needed in order to fit the data for fission induced by light ions.

The pion optical model has given excellent fits[21] to elastic scattering data for a range of targets at incident pion energies below 100 MeV. This model has also been used recently[28] to calculate with reasonable success true pion absorption cross sections, σ_{abs}, for a range of targets. For the present calculations, the pion optical model calculations from the code DWPIES (Ref. 29) provided the σ_{abs} and the σ_R for pions incident on ^{238}U. The excitation energy of the fissioning system will differ greatly depending on whether the incident pion was absorbed or inelastically scattered. The division of σ_R into σ_{abs} and a quasielastic part, σ_{qe}, using the pion optical model (see the Appendix), gives the necessary information from which to calculate the contribution to σ_F from high or moderate excitation. Once the contributions are known, the exciton model[25] can be used to bring the nucleus to thermal equilibrium. The exciton model is incorporated in the ALICE program via the preequilibrium nucleon emission option. The preequilibrium parameters used were taken from a study for stopped π^- by Blann.[30] The results of these calculations are presented in Figs. 8(a) and (b) for two values of the level density ratio. As for the cascade calculations, the DWPIES-ALICE calculations, as shown in Fig. 8(a), predict σ_F to be nearly equal for π^+ and π^- when $R = 1$ is used. Again, much better agreement with the data is obtained for $R = 1.1$ as shown in Fig. 8(b). These calculations do marginally better than those shown in Fig. 7(b) in reproducing the energy-dependent total fission cross sections.

The DWIPES-ALICE calculations were also used to predict the mass dependence of the fission cross sections. The values of σ_F for ^{238}U and ^{209}Bi at 80 MeV from data set B, and the renormalized values for ^{197}Au at 78 MeV

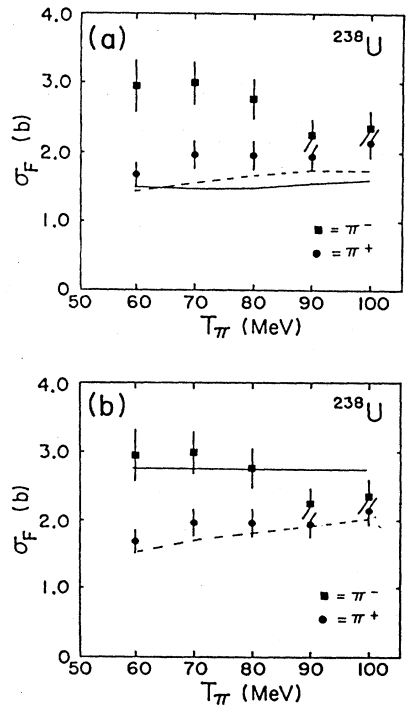

FIG. 8. Comparison of the fission cross section for ^{238}U to calculations for π^- (solid line) and π^+ (dashed line) using the DWPIES and ALICE codes with values of the level density ratio $R = a_f/a_\nu$ equal to (a) 1.0 and (b) 1.1.

from data set A are shown in Fig. 9 along with calculations for several values of $R = a_f/a_\nu$. Here a value of $R = 1.1$ does not do well. The best description of the data is obtained for $R \simeq 1.03$. Although this result disagrees with the value of R needed for ^{238}U, an earlier study[20] for 45 MeV ^{3}He also finds a best fit to the data for $R \simeq 1.03$ when the Z^2/A dependence of σ_F is examined. We conclude that, as before, the basic statistical fission parameters must be modified in the same way needed to fit the data from fission induced by light ions in order to describe our data. The difference between the value of R obtained for ^{238}U fission cross sections and that for a general range of Z and A might be attributed to differences in the nuclear structure of the different targets (such as the ground state deformation) or may be due to problems in calculating fission barriers using the rotating liquid drop model.

A direct comparison between the values of σ_F for ^{238}U from data set B with other published reaction cross section data can be made using the approximation $\sigma_F \simeq \sigma_R$. This approximation is expected, on the basis of light-ion-induced fission,[9,31] to be quite good for π^+ incident on ^{238}U, and fairly good for incident π^-. The data of Ashery *et al.*[1] and Navon *et al.*[32] for ^{209}Bi are plotted in Fig. 10 along with pion total cross sections for ^{208}Pb from Carroll *et al.*[33] and the σ_F for ^{238}U. Only for π^+ at 85 MeV may a direct comparison be made between σ_R and σ_F. In this case, the σ_R is about 50% higher than the corresponding σ_F. However, the large uncertainty for the inelastic cross section measured by Ref. 1 ($\sigma_{\text{inel}} = 1.18 \pm 0.92$ b) makes any definite conclusion difficult. At 50 MeV, the σ_{abs} for π^- of Ref. 32 is almost a factor of 2 above the 60 MeV π^- σ_F for ^{238}U. It seems rather unlikely that pion absorption would not lead to fission of ^{238}U, and the σ_{abs} for ^{238}U should be slightly larger than the σ_{abs} for ^{209}Bi. In addition, the σ_{abs} for π^- from Ref. 32 is very close to the measured total cross section, σ_T, of Ref. 33, whereas about half of the σ_T is expected to be made up of elastic scattering. Both the σ_F and σ_T comparisons indicate that the σ_{abs} reported in Ref. 32 is too high and should be checked by further measurement.

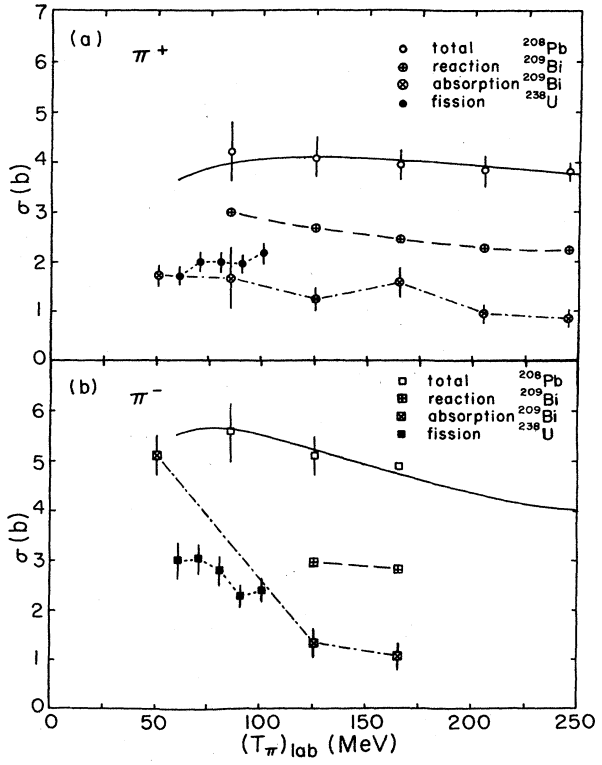

FIG. 10. Comparison of the measured fission cross sections for ^{238}U with other pion-nucleus cross section data on heavy nuclei. The total cross sections and the solid curves are from Ref. 33. The absorption cross sections at 50 MeV are from Ref. 32; the absorption cross sections at higher energies and the reaction cross sections are from Ref. 1. The uncertainties on the reaction cross section data are large and not shown.

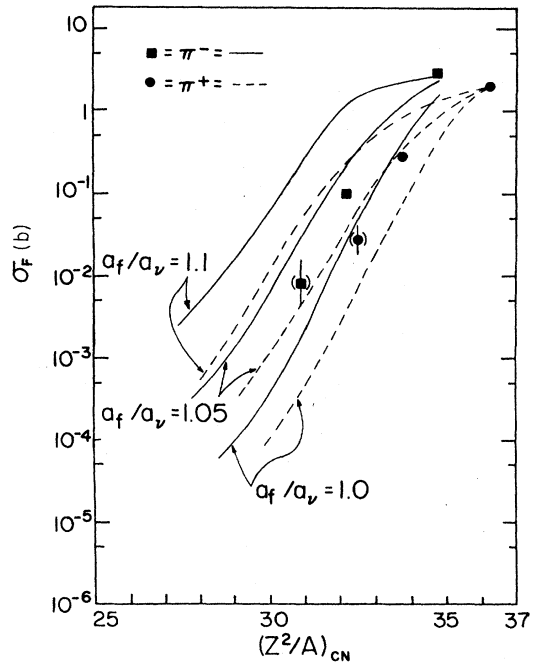

FIG. 9. Total fission cross sections at 80 MeV as a function of the compound nucleus Z^2/A along with calculations using the DWPIES and ALICE codes for several values of the level density ratio a_f/a_ν. The points in parentheses are normalized from data set A as described in the text.

V. CONCLUSIONS

The present study has revealed information on at least two important points. First, measurements of σ_F can establish approximate σ_R for pion interactions with heavy nuclei; these σ_R are not yet completely determined from other experiments. Second, some insight has been obtained on coupling of the pion-nucleus interaction to collective modes of the nucleus.

Few differences between fission induced by pions and

by nucleons or light ions were seen. The excitation energy of the fissioning system was deduced in the model given by Nix,[8] with the indication that most of the fission comes from compound nuclei with excitation energies greater than 100 MeV for pion kinetic energies of 60 to 100 MeV. This requires that true absorption of the pion is a main contributor to the fission measured in our study. One significant difference seen is that the mass distributions are significantly wider for pion-induced fission than for conventional fission at a similar excitation energy. At present, no satisfactory explanation for this phenomenon is apparent.

The total fission cross sections have similar magnitude (see Fig. 6) for pion-induced fission at 80 MeV and proton-induced fission at 156 and 190 MeV. Calculations of the σ_F in our study have resulted in conclusions similar to those drawn from light-ion-induced fission. The level density ratio, $R = a_f/a_\nu$, must be increased from the simplest value of $R = 1.0$ to $R \geq 1.1$ for fission of ^{238}U, and to $R \sim 1.03$ in order to reproduce the σ_F as a function of Z^2/A.

ACKNOWLEDGMENTS

We thank T. G. Masterson, J. H. Mitchell, and W. Tew for assisting with the measurements, and Clayton Olson of Los Alamos for preparing the ^{238}U target. Many other members of the staff at Los Alamos also provided valuable assistance. The program DWPIES and assistance in its use were furnished by E. Siciliano. M. Blann is especially thanked for providing the ALICE program and much helpful advice on statistical fission theory. We thank L. C. Lui for making available the ISOBAR code. This work was supported in part by the United States Department of Energy and the National Science Foundation.

APPENDIX

Only part of the imaginary optical potential for pions represents true absorption. In this appendix we demonstrate how the cross section due to such true absorption may be computed.

In order to calculate the reaction cross section one starts from the wave equation to derive the continuity equation. This gives the time rate of flux loss in a volume as

$$W = -\frac{2}{\hbar}\langle \Psi^+ \mid \mathrm{Im}V \mid \Psi^+ \rangle ,$$

where Ψ^+ satisfies the boundary condition (with no Coulomb potential)

$$\Psi^+ \rightarrow e^{i\mathbf{k}\cdot\mathbf{r}} + f(\theta)e^{ikr}/r .$$

For a potential of the form[2,28]

$$(2E/\hbar^2)V\Psi^+ = -f(r)\Psi^+ + \nabla\cdot g(r)\nabla\Psi^+ ,$$

the reaction cross section is expressed as

$$\sigma_R = (E/\hbar k)W$$
$$= \frac{1}{k}[\langle \Psi^+ \mid \mathrm{Im}f(r) \mid \Psi^+ \rangle + \langle \nabla\Psi^+ \mid \mathrm{Im}g(r) \mid \nabla\Psi^+ \rangle] .$$

The first term can be evaluated numerically in a straightforward fashion by using the partial wave expansion

$$\Psi^+ = \sqrt{4\pi}\sum_l \sqrt{2l+1}\, i^l \frac{u_l(kr)}{kr} Y_{lm}(\theta,\phi) .$$

The second term makes use of the relation

$$\nabla\Psi^+ = \hat{\mathbf{r}}\hat{\mathbf{r}}\cdot\nabla\Psi^+ - i\frac{\hat{\mathbf{r}}\times\mathbf{L}\Psi^+}{r} ,$$

where $\mathbf{L}$ is the angular momentum operator. With some simplifications the expression for the reaction cross section becomes

$$\sigma_R = \frac{4\pi}{k^2}\sum_l (2l+1)\,\mathrm{Im}\left\{\int_0^\infty \left[f(r) + \frac{l(l+1)}{r^2}g(r)\right] \times |u_l(r)|^2 dr + \int_0^\infty g(r)\left|\frac{du_l}{dr} - \frac{u_l}{r}\right|^2 dr\right\} .$$

The shape factors for the potentials are divided into one part which represents the quasielastic processes and one which represents the true absorption:

$$f(r) = f_{\mathrm{qe}}(r) + f_{\mathrm{abs}}(r)\ (\mathrm{real}) ,$$
$$g(r) = g_{\mathrm{qe}}(r) + g_{\mathrm{abs}}(r) + (\mathrm{imaginary}) .$$

Since the reaction cross section is linear in the imaginary potentials, the true absorption cross section, σ_{abs}, may be calculated by substituting only the imaginary potential which represents the true absorption into the above expression. The necessary integrals are calculated numerically using the distorted wave functions calculated in the DWPIES (Ref. 29) program.

*Present address: TRIUMF, 4004 Wesbrook Mall, Vancouver, British Columbia, Canada V6T 2A3.

†Present address: University of Michigan Group, Brookhaven National Laboratory, Upton, NY 11973.

[1]D. Ashery, I. Navon, G. Azuelos, H. K. Walter, H. J. Pfeiffer, and F. W. Schlepütz, Phys. Rev. C **23**, 2173 (1981); D. Ashery *et al.*, Phys. Rev. Lett. **42**, 1465 (1979).

[2]K. Stricker, H. McManus, and J. A. Carr, Phys. Rev. C **19**, 929 (1979).

[3]M. B. Johnson and E. R. Siciliano, Phys. Rev. C **27**, 730 (1983); **27**, 1647 (1983).

[4]R. Vandenbosch and J. R. Huizenga, *Nuclear Fission* (Academ-

ic, New York, 1973).
[5]G. F. Denisenko *et al.*, Phys. Rev. **109**, 1779 (1958).
[6]Yu. A. Batusov *et al.*, Yad. Fiz. **23**, 1169 (1976) [Sov. J. Nucl. Phys. **23**, 621 (1976)]; B. Budick *et al.*, Phys. Rev. Lett. **24**, 604 (1970).
[7]P. Hecking, Phys. Lett. **103B**, 401 (1981).
[8]J. R. Nix, Nucl. Phys. **A130**, 241 (1969).
[9]V. E. Viola, Jr. *et al.*, Phys. Rev. C **26**, 178 (1982).
[10]H. R. Bowman *et al.*, Phys. Rev. **168**, 1396 (1968).
[11]C. S. Zaidins, J. B. Martin, and F. M. Edwards, Med. Phys. **5**, 42 (1978).
[12]G. W. Butler *et al.*, Phys. Rev. C **26**, 1737 (1982).
[13]B. E. Fischer and R. Spohr, Rev. Mod. Phys. **55**, 907 (1983).
[14]Manufactured by DuPont and available from VWR Scientific.
[15]F. Plasil *et al.*, Phys. Rev. **142**, 696 (1966).
[16]J. A. Wheeler, in *Fast Neutron Physics,* edited by J. Marion and J. Fowler (Interscience, New York, 1963); P. D. Bond, Phys. Rev. Lett. **52**, 414 (1984).
[17]J. J. Griffin, in *Proceedings of the International Energy Agency Symposium on Physics and Chemistry of Fission, Vienna, 1965* (IAEA, Vienna, 1966), Vol. 1, p. 23; V. E. Viola, Jr., Nucl. Data **A1**, 391 (1966).
[18]V. E. Viola, Jr., Nucl. Data **A1**, 391 (1966).
[19]P. C. Stevenson, H. G. Hicks, W. E. Nervik, and D. R. Nethaway, Phys. Rev. **111**, 886 (1958).
[20]F. D. Becchetti, K. H. Hicks, C. A. Fields, R. J. Peterson, R. S. Raymond, R. A. Ristinen, J. L. Ullmann, and C. S. Zaidins, Phys. Rev. C **28**, 1217 (1983).
[21]K. Stricker, J. A. Carr, and H. McManus, Phys. Rev. C **22**, 2043 (1980).
[22]M. Maurette and C. Stephan, in *Proceedings of the International Atomic Energy Agency Symposium on Physics and Chemistry of Fission, Vienna, 1968* (IAEA, Vienna, 1969), Vol. 2, p. 307.
[23]F. D. Becchetti, J. Janecke, P. Lister, K. Kwiatkowski, H. Karwowski, and S. Zhou, Phys. Rev. C **28**, 276 (1983).
[24]M. Blann and J. Bisplinghoff, Lawrence Livermore National Laboratory Report UCID-19614, 1982 (unpublished).
[25]M. Blann, Annu. Rev. Nucl. Sci. **25**, 123 (1975).
[26]Z. Fraenkel, E. Piasetzky, and G. Kalbermann, Phys. Rev. C **26**, 1618 (1982).
[27]M. Blann and T. T. Komoto, Phys. Rev. C **29**, 1678 (1984).
[28]J. A. Carr, H. McManus, and K. Stricker-Bauer, Phys. Rev. C **25**, 952 (1982).
[29]E. R. Siciliano (private communication). Program DWPIES is a modified version of DWPI; R. A. Eisenstein and G. A. Miller, Comput. Phys. Commun. **11**, 95 (1976).
[30]M. Blann, Phys. Rev. C **28**, 1648 (1983).
[31]W. G. Meyer *et al.*, Phys. Rev. C **20**, 1716 (1979).
[32]I. Navon, D. Ashery, J. Alster, G. Azuelos, B. M. Barnett, W. Gyles, R. R. Johnson, D. R. Gill, and T. G. Masterson, Phys. Rev. C **28**, 2548 (1983).
[33]A. S. Carroll *et al.*, Phys. Rev. C **14**, 635 (1976).